Observation of Carbon Nanotube and Clay Micellelike Microstructures with Dual Dispersion Property

Yi-Fen Lan and Jiang-Jen Lin*

Institute of Polymer Science and Engineering, National Taiwan University, Taipei 10617, Taiwan

Received: March 24, 2009; Revised Manuscript Received: June 19, 2009

Micellar microstructures of carbon nanotubes (CNTs) with clay platelets were formed by physically pulverizing both materials in powder form. The resultant CNT−clay mixtures were enabled to decrease the level of aggregation of the CNTs from their original state in water as well as in organic mediums including toluene, dimethylformamide, and ethanol. The presence of clay significantly enhanced the CNT dispersion in the following trend: anionic synthetic fluorinated mica ($300 \times 300 \times 1$ nm^3) > anionic sodium montmorillonite ($80 \times 80 \times 1$ nm^3) > cationic layered double hydroxide ($200 \times 200 \times 1$ nm^3). Both geometric dimensions and ionic charge could be the predominant factors for decreasing the CNT entanglement. The CNT−Mica demonstrated an amphiphilic property for dispersing in water and toluene, but in an irreversible manner. It is explained that the original CNT and clay's noncovalent bonding forces are randomized during the contact with solvent. The formation of micellelike microstructures, resembling oil-in-water and water-in-oil surfactants, was proposed. Ultraviolet−visible absorbance and transmission electronic microscopy have verified the existence of two different microstructures, which also exhibited differences in thermal stability (600 vs 650 °C onset temperature) by thermal gravimetric analysis as well as electrical conductivity (10^{-4} vs 10^{-6} S/cm).

Introduction

Carbon nanotubes (CNTs) are expected to exhibit superior chemical and physical properties because of their high aspect ratio dimension and the conjugated character of individual tubes.[1−4] Due to their unique conducting properties, numerous applications were demonstrated.[5−8] However, the tube-shaped CNTs tend to aggregate through their lengthy geometric shape and strong van der Waals force attraction, which may consequently hinder their uses in many applications. To overcome these problems, covalent functionalization was proposed to improve the CNT dispersion or reduce their aggregation. The following approaches are commonly used to functionalize CNTs: oxidation,[9,10] atom transfer radical polymerization,[11,12] acylation-mediated amidation,[13,14] and carbodiimide-activated coupling.[15,16] Nevertheless, most of these processes involve an organic covalent bonding reaction which consequently destroys the sp^2 structure in the graphite sheet. Hence, the covalent-bonding modification may be disadvantageous due to the possible destruction of the unique CNT structure. Alternative methods by using noncovalent bonding modification are desired. Suitable surfactants,[17−19] polymers,[20−22] and biomolecules[23−25] are commonly applied for the CNT surface interactions for the purpose of easy dispersion. More recently, room-temperature ionic liquids were found to be effective for dispersing CNTs by physical grinding to form gels through cation−π interaction.[26,27]

Herein, we reveal a unique nature of dispersing behavior for a pulverized CNT/clay mixture and development of a convenient method for minimizing the CNT aggregation without using organic dispersants. In particular, a synthetic fluorinated mica clay is most effective due to its large plate size and anionic property. Through the simple physical mixing of two nanomaterials of different geometric shapes, tubelike CNT and platelike silicate clays, the mutual interaction affects their inherent self-aggregating forces. The CNT−clay hybrid is dispersible in most common organic solvents including water and toluene. The possible formation of micellelike microstructures of the CNT−clay mixture is postulated and their existence is indirectly proven by measuring thermal and electronic properties. A mechanism involving the factor of geometric-shape difference and mutual exclusion of noncovalent bonding interaction among the pristine nanoparticles is proposed to account for this dispersion preference.

Experimental Section

Materials. Carbon nanotubes were supplied by Seedchem Company Pty., Ltd., and prepared from chemical vapor deposition. The CNTs are 95% pure containing 5% catalyst (Fe, Co, and Ni). The dimensions of a CNT are 40−60 nm in diameter and 0.5−10 μm in length. To realize the influence of the aspect ratio of layered silicate clays, three kinds of clays were selected for comparison. Synthetic fluorinated mica (Mica) was obtained from CO-OP Chemical Co. (Japan). Sodium montmorillonite (MMT) was supplied from Nanocor Co. The geometric structures of the pristine anionic clays, Mica and MMT, are irregularly aggregated with the primary units consisting of silicate platelets in stacks.[28] The unit platelets are irregularly shaped and have ionic charges with $\equiv SiO^-Na^+$. Their average dimensions were estimated to be approximately $80 \times 80 \times 1$ nm^3 for MMT and $300 \times 300 \times 1$ nm^3 for Mica. Due to the presence of an intensive ionic charge character, these clays are hydrophilic and swelling or gelling in water.[29] With similar platelet structure but a charge-opposite cationic character, the clay of $[Mg_6Al_2(OH)_{16}]CO_3 \cdot 4H_2O$ (layered double hydroxide, LDH) was prepared for comparison. The Mg−Al LDH is a clay with cationic layers which are balanced by anions such as carbonate and water molecules.[30,31] LDH clay with an average dimension of $200 \times 200 \times 1$ nm^3 was prepared according to the procedures reported previously in our laboratories.[32]

* Corresponding author. Telephone: +886-2-3366-5312. Fax: +886-2-3366-5237-4159. E-mail: jianglin@ntu.edu.tw.

10.1021/jp9026805 CCC: $40.75
Published on Web 07/09/2009

Preparation of CNT−Mica Hybrid. The procedure of mixing Mica−CNT hybrid is exemplified below. CNTs (1 mg) and Mica (1 mg) were ground adequately in an agate mortar and pestle. The sides of the mortar were occasionally scraped down with the pestle during grinding to ensure a thorough mixing. The mixture was washed from the mortar and pestle using deionized water at concentration of 1 mg of CNTs in 20 g of water. The Mica−CNT hybrids were prepared at clay-to-CNT weight ratios, or α values, of 0.33, 0.5, 1, 2, and 3.

Amphiphilic Dispersion in Organic Solvents or Water. Ternary mixtures of the Mica−CNT hybrid were examined for the dispersion ability in water and toluene in different orders of addition. In the first example, the hybrid of Mica−CNT (2.0 mg/1.0 mg or α = 2) was added to 7.5 g of water first, thoroughly dispersed, and then added to 7.5 g of toluene. In the second example, the hybrid was dispersed in toluene, homogeneously mixed, and then added to water. During the mixing, ultrasonic vibration was applied for 2 min. Ultrasonication was operated on a BRANSON 5510R-DTH (135 W, 42 kHz).

Characterization. Ultraviolet−visible (UV−vis) absorbance was measured by a Perkin-Elmer Lambda 20 UV−vis spectrophotometer at 550 nm. Transmission electron microscopy (TEM) was performed on a Zeiss EM 902A at 120 kV. Samples were prepared by drop-coating sample solution (0.01 wt %) on a copper target and evaporation under vacuum at ambient temperature for 1 h. Field emission scanning electron microscopy (FE-SEM) images were obtained from a JEOL JSM-6700F SEM system. The samples were coated with Au before the FE-SEM measurements. Thermal gravimetric analysis (TGA) was performed on Perkin-Elmer Pyris 1 TGA from 100 to 900 °C in air to examine the thermal stability of clay−CNT hybrid. The conductivity of the hybrid was measured by a four-terminal technique (ASTM F390). The preparation of standard specimens for conductivity is described as following. The clay−CNT hybrid (α = 2) was dispersed in toluene or water, dropped on a glass surface (20 × 20 mm), and then dried in an oven at 80 °C.

Results and Discussion

Clays Affecting the CNT Aggregation. The tubelike CNTs are composed of conjugated sp^2 orbital bonds. Due to the high aspect ratio dimensions of 40−60 nm diameter and 0.5−10 μm length, the materials tend to aggregate and are difficult for solvating into water or organic solvents. The self-aggregation and entanglement are mainly caused by van der Waals force attraction. However, when CNTs were properly ground with platelike clays such as the fluorinated mica, the pulverized powders as a physical mixture became readily dispersible in water. The grinding procedure for the preparation can be monitored by the FE-SEM image. As shown in Figure 1, the heterogeneous mixtures were observed after grinding 1 min (Figure 1a), and homogeneity was obtained after grinding 5 min (Figure 1b).

The CNT aggregation was significantly minimized by compounding CNT with the clays at varied weight ratios. Initially, it was found that the Mica with CNT at 2:1 weight ratio, or α = 2 (defined as the weight ratio of clay to CNT), could render the mixtures easily dispersible in water to generate a fine slurry. The fine dispersion can be differentiated by the naked eye as a black suspension from solid precipitates in the bottom layer (Figure 1c). The controlled experiments showed that the pristine CNTs were not dispersible in water but formed severe aggregates. The efficacy for the CNT dispersion depends on the relative amount of the Mica. The black CNTs were mostly precipitated at the bottom of the water phase when a lesser amount of Mica to CNT was used at α = 1−0.5. It appears that the presence of Mica may mitigate the formation of CNT aggregates.

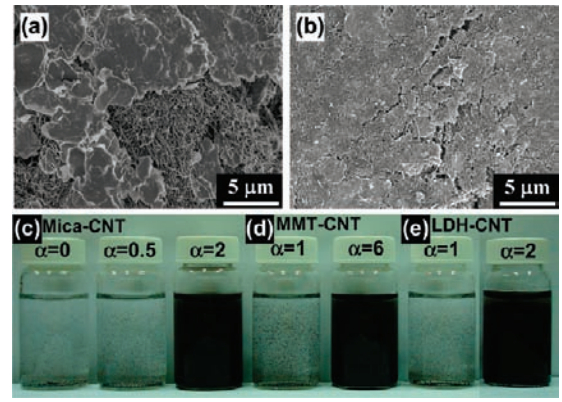

Figure 1. FE-SEM of CNTs and Mica under pulverizing for (a) 1 and (b) 5 min. Visual observation of the dispersion of clay−CNT hybrids in water: (c) Mica−CNT, (d) MMT−CNT, and (e) LDH−CNT, under varied α value (α = clay/CNT weight ratio). Each sample contained 1 mg of CNTs in 20 g of water.

In order to understand the nature of Mica−CNT interaction, two other clays including MMT and the cationic type of LDH were further examined. The use of different clays in geometric dimensions and charges, for example, Mica (300 × 300 × 1 nm^3), MMT (80 × 80 × 1 nm^3), and LDH (200 × 200 × 1 nm^3), allow the understanding of their size effect for the CNT dispersion in water. In Figure 1d,e, the photographs illustrate the fine CNT dispersion obtained by the addition of MMT at α = 6 (or 6 times the clay weight to CNTs). For comparison, Mica is more effective than MMT under the same agitating condition of mechanical stirring or shaking. These results indicate that the platelet size may be the dominating factor for the fine dispersion. The dispersion was further measured by analyzing the suspension using UV−visible spectrometry. As shown in Figure 2a, the absorbance at 550 nm for the CNTs becomes more intense with the increasing amount of added Mica, implying the increase of CNT content in water.[33,34] Experimentally, the comparison of dispersing ability by the UV−visible absorbance is plausible since the absorbance actually correlates well with the hybrid concentration by following the Lambert−Beer law.[35,36] The standard curves of absorbance against concentration were established at 550 nm (Figure 2b) for the hybrids using three different clays. According to the UV−vis analysis in Figure 2a, the Mica is most effective for enhancing the CNT dispersion in water. The absorbance reached a maximum when the Mica−CNT weight ratio approached α = 2−3, but required a higher α value of 6 for the comparative MMT. In considering their ionic charges, the LDH is ionic, with cationic charges on the platelet surface and nitrate anionic species as the counterions. The ionic charge interaction between CNTs and clay, through the clay surface anions (≡SiO^-) in MMT and Mica structures or cations in LDH, may be the second reason for affecting the CNT dispersion. The apparent dispersing experiments indicated that LDH was also effective but required additional ultrasonic agitation during mixing as shown in Figure 2b (LDH−CNT). In general, ultrasonic vibration was found to be able to provide additional agitation energy. The dispersion of Mica−CNT was further examined by TEM (Figure 2c,d), showing a rather fine dispersion in water in contrast to that of the pristine CNT.

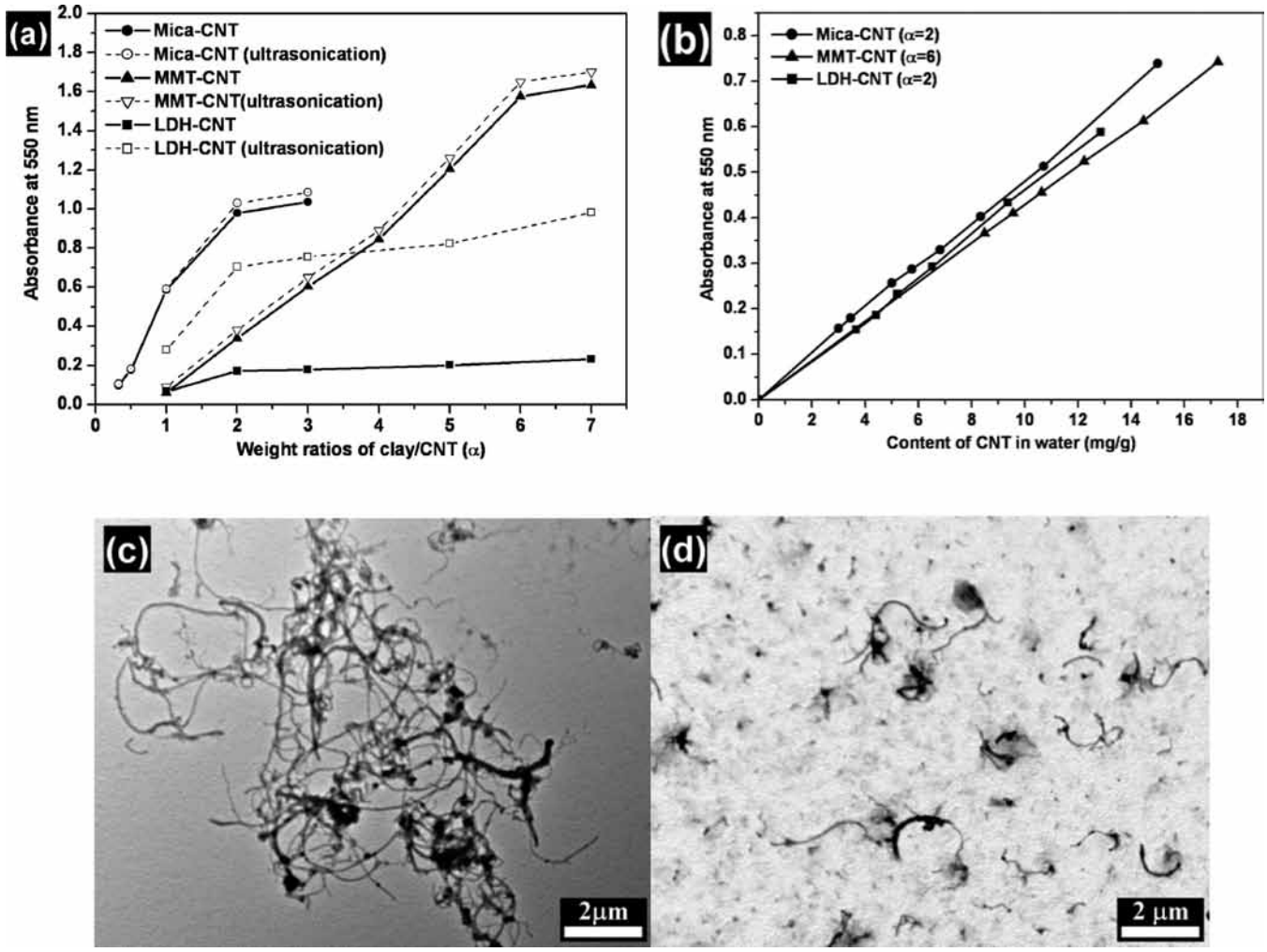

Figure 2. (a) UV−vis absorbance of clay−CNT at different α values of hybrids in water. (b) Three standard curves of clay−CNT hybrids at different CNT content. The increase of UV−vis absorbance in (a) indicated the dispersing ability of the clay species improvement of CNT dispersion in reference to the standard curves in (b) of absorbance vs CNT in water. In TEM (c and d), the pristine CNT showing serious aggregates and a loose dispersion for CNT−Mica (at $\alpha = 2$) at low concentration of 10^{-4} wt % CNT.

The role of Mica in assisting the CNT dispersion in other mediums was also investigated. It is known that CNTs are only sluggishly dispersible in organic solvents such as DMF, but precipitate in water and solvents such as ethanol and toluene. In contrast, inorganic clay materials such as MMT and LDH are generally hydrophilic and swollen in water, but lack dispersing ability in most organic mediums. However, due to the presence of the fluorinated functionality, the synthetic Mica is actually amphiphilic or behaves with a dual dispersing property in water as well as in most common solvents, such as ethanol, acetone, dimethylformamide, and toluene. As summarized in Table 1, Mica and MMT could generally affect the CNT dispersion in most organic mediums. For example, the pulverized Mica−CNT hybrid at $\alpha = 2$, after thorough grinding and ultrasonic agitation, became dispersible for most organic solvents. It appears that the presence of Mica actually affects the CNT self-entanglement through interaction with the involved medium.

Amphiphilic Property for Dispersion. Being dispersible in both water and toluene, the Mica−CNT hybrid ($\alpha = 2$) is considered to be amphiphilic in nature. This dual hydrophilic/hydrophobic dispersion behavior was further shown to be in an irreversible manner. Figure 3a shows the grinding procedure of preparation of Mica−CNT hybrid. The hybrid was dispersed in water first and then toluene was added; after shaking and allowing settlement, the black Mica−CNT remained in the water phase (Figure 3b). In contrast, if the same hybrid powder was dispersed in toluene first, a toluene suspension remained in the toluene phase even after vigorous agitation with water (Figure 3c). The order of solvent exposure to either water or toluene determined the hybrid's preference in an irreversible manner (Supporting Information, movies S1 and S2). The phenomenon is explainable by adopting the concept of stable "micellelike" microstructures, the formations of water-in-oil (W/O) and oil-in-water (O/W) phases as shows in Figure 4e.

Regarding the nature of "micellelike" microstructures, both types of dispersions in water and toluene were analyzed by

TABLE 1: Dispersion of CNT, Mica, and the Hybrid in Various Mediums

solvent	Mica[a]	MMT[a]	CNT[b]	Mica−CNT[c]
H_2O	+	+[d]	−[e]	+
ethanol	+	−	−	+
acetone	+	−	−	+
DMF	+	−	+	+
toluene	+	−	−	+

[a] Mica or MMT, 2 mg in 20 g of solvent. [b] CNT (1 mg) in 20 g of solvent. [c] Mica−CNT (2.0 mg/1.0 mg or $\alpha = 2$) dispersed in 20 g of solvent. [d] +, good dispersion. [e] −, poor dispersion or precipitation.

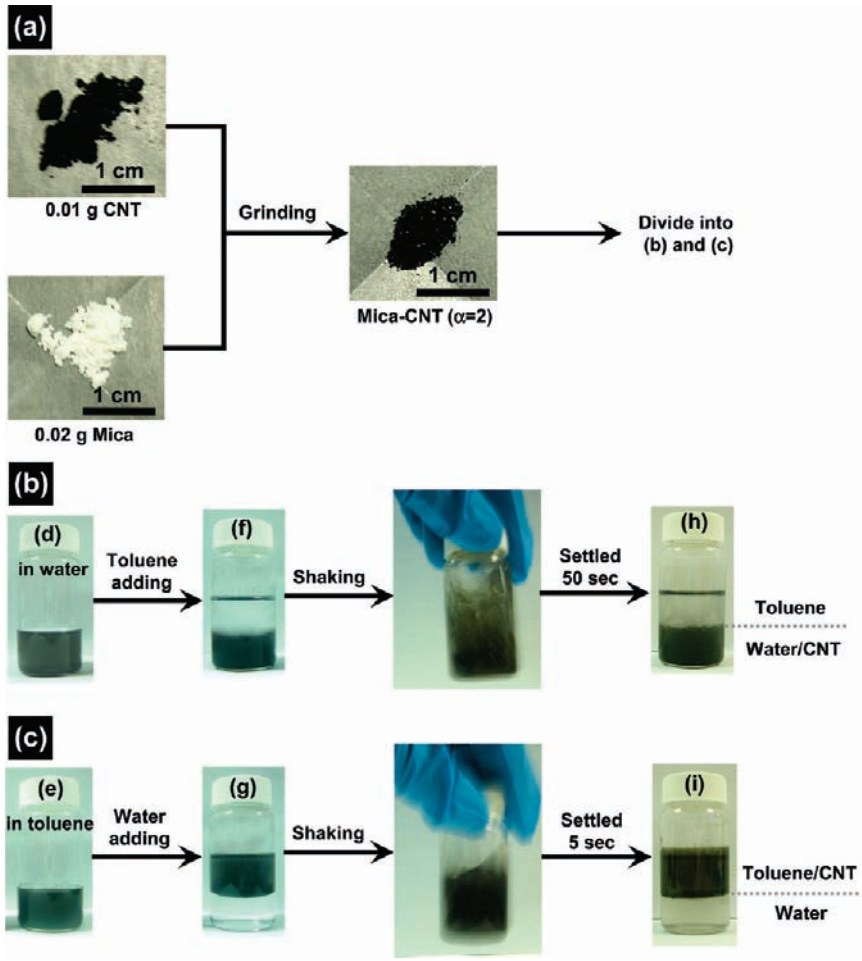

Figure 3. Irreversible dispersion phenomenon of Mica−CNT at $\alpha = 2$. (a) Grinding procedure of Mica−CNT hybrid. Hybrid was dispersed in either water (d) or toluene (e); both dispersions remained in the original solvent after adding the other solvent (f and g). After vigorous shaking, the dispersion settled into distinct layers in an irreversible manner (h and i).

using TEM, TGA, and a device of electrical conductivity. At a low concentration of CNT dispersion (10^{-4} wt %) in water, the TEM images showed a better CNT−Mica hybrid dispersion in water while a large aggregation was observed for the pristine CNT as shown in Figure 2c,d. At a higher concentration such as 10^{-3} wt % CNT, different morphologies of microstructures were identified. For example, more visible Mica platelets of micrometer size aggregation were found for the hybrid being exposed to water (Figure 4a,b). On the contrary, when the same Mica−CNT hybrid was dispersed in toluene, the CNT aggregates appeared to be on the surface of microstructures (Figure 4c,d). On thermal stability, the Mica−CNT hybrid exhibited different decomposition patterns when being exposed to water or toluene. The hybrid after dispersing in water is thermally more stable than that in toluene. There is a 50 °C difference in the decomposition patterns for delaying the weight loss (Figure 5). It appears that the Mica surrounding CNTs in an O/W microstructure may have a shielding effect for the CNT decomposition, in comparison with the naked CNTs in the W/O hybrid. Furthermore, the micellelike microstructures can be further indirectly evidenced by the performance of conductivity. When the hybrid was coated on the glass substrate, the specimen from toluene suspension had a higher conductivity at 10^{-4} S/cm than that from water suspension, at 10^{-6} S/cm. The result of the 2 order of magnitude difference is derived from the same batch of pulverized powder ($\alpha = 2$). Hence, two forms of W/O and O/W types or different arrangements of CNT-in-Mica and Mica-in-CNT microstructures are indirectly evidenced.

Explanation for the Formation of Mica−CNT Microstructures. The formation of two Mica−CNT microstructures is attributed to the randomization of the noncovalent bonding forces among individual CNTs and clays in different hydrophilic water or hydrophobic toluene mediums. The initial grinding of two nanomaterials, tubelike CNTs and platelike clay, could largely redistribute the original CNT self-aggregation. Their CNT entanglement force may be mitigated or blocked by the neighboring platelets due to the difference in their geometric shapes. Furthermore, since the clay is hydrophilic, contact with water could render the hybrid to form an O/W microstructure, comprising CNTs as the core and Mica as the surrounding corolla. Similarly, the opposite water-in-oil (W/O) or Mica-in-CNT microstructures is possibly generated since the CNTs favored the toluene in the continuous phase. Two different types of microstructures could be generated and stabilized through vigorous agitation in the selected solvent.

Conclusion

The aggregating behavior of CNTs in various organic mediums or in water was significantly reduced by simply grinding CNTs with clays into fine powder. In particular, the CNT dispersion in water and toluene was significantly enhanced by Mica that was more effective than MMT or LDH

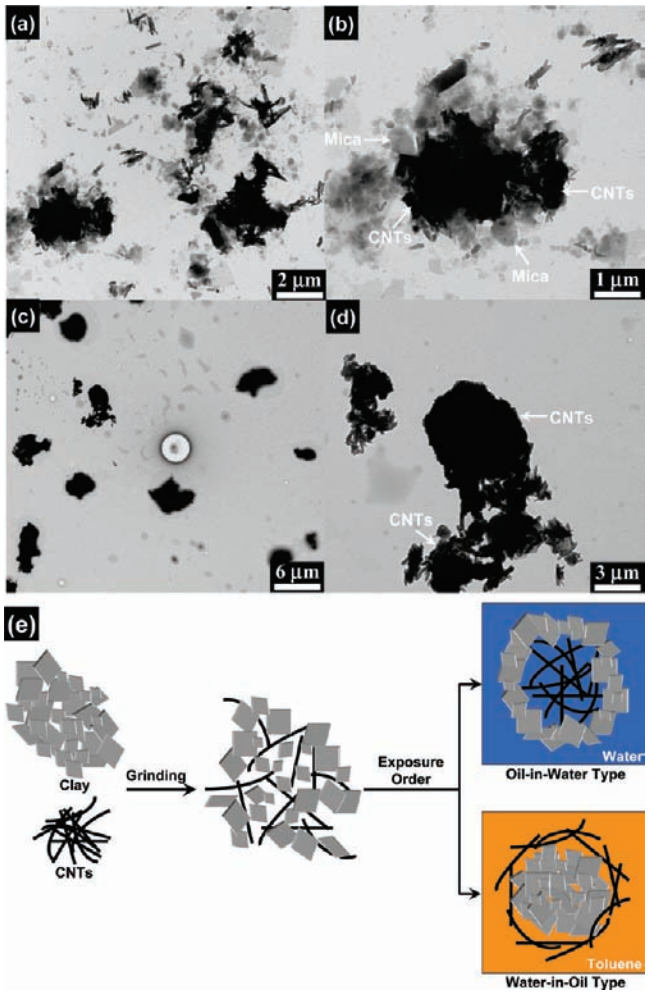

Figure 4. TEM images of Mica−CNT hybrid dispersed in water (a and b) and in toluene (c and d) at 10^{-3} wt % CNT. Mica−CNT hybrid was obtained from the same batch; however, hybrid has completely different microstructures when exposed to water or toluene. In water, hybrid shows more Mica appearance; on the contrary, more hairy CNT composition was observed. Conceptual illustration (e) shows the mixing of the two materials and their possible oil-in-water (O/W) and water-in-oil (W/O) microstructures.

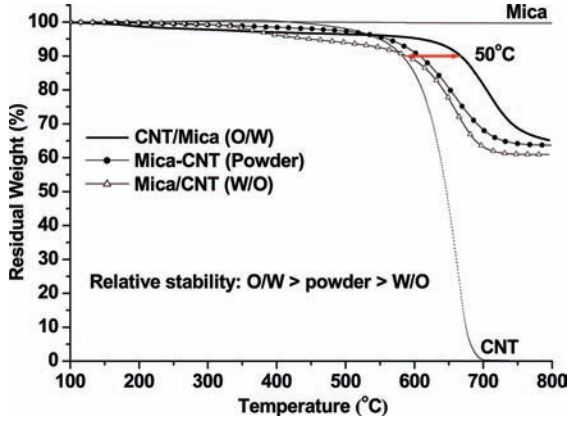

Figure 5. TGA patterns for pristine CNT, Mica, and their hybrid ($\alpha = 2$). Mica−CNT (pulverized powder); Mica−CNT (O/W), with the hybrid being dispersed in water and dried; Mica−CNT (W/O), with the hybrid being dispersed in toluene and dried.

because of its high aspect ratio geometric shape and anionic character. A mechanism involving the formation of CNT−Mica and Mica−CNT micellelike microstructures, resembling the organic surfactants in oil-in-water and water-in-oil forms, is proposed. The existence of two different microstructures was indirectly evidenced by observing the differences in thermal stability due to the Mica shielding in CNT-in-Mica microstructure and variable electrical conductivity (10^{-4} vs 10^{-6} S/cm). The clay-assisted CNT dispersion in water without using an organic dispersant may offer significant advances for CNT applications.

Acknowledgment. We acknowledge financial support from the National Science Council (NSC) and the Ministry of Economic Affairs, Taiwan.

Supporting Information Available: Two movies showing the irreversible dispersion in water and toluene. This material is available free of charge via the Internet at http://pubs.acs.org.

References and Notes

(1) Pang, S. K.; Saxby, J. D.; Chatfield, S. P. *J. Phys. Chem.* **1993**, *97*, 6941–6942.
(2) Lu, J. P. *Phys. Rev. Lett.* **1995**, *74*, 1123–1126.
(3) Dai, H.; Wong, E. W.; Lieber, C. M. *Science* **1996**, *272*, 523–526.
(4) Rao, A. M.; Eklund, P. C.; Bandow, S.; Thess, A.; Smalley, R. E. *Nature* **1997**, *388*, 257–259.
(5) Liu, J.; Tian, S.; Knoll, W. *Langmuir* **2005**, *21*, 5596–5599.
(6) Kim, K.; Lee, S. H.; Yi, W.; Kim, J.; Choi, J. W.; Park, Y.; Jin, J. I. *Adv. Mater.* **2003**, *15*, 1618–1622.
(7) So, H. M.; Won, K.; Kim, Y. H.; Kim, B. K.; Ryu, B. H.; Na, P. S.; Kim, H.; Lee, J. O. *J. Am. Chem. Soc.* **2005**, *127*, 11906–11907.
(8) Tian, Z. Q.; Jiang, S. P.; Liang, Y. M.; Shen, P. K. *J. Phys. Chem. B* **2006**, *110*, 5343–5350.
(9) Liu, J.; Rinzler, A. G.; Dai, H.; Hafner, J. H.; Bradley, R. K.; Boul, P. J.; Lu, A.; Iverson, T.; Shelimov, K.; Huffman, C. B.; Fernando, R. M.; Shon, Y. S.; Lee, T. R.; Colbert, D. T.; Smalley, R. E. *Science* **1998**, *280*, 1253–1256.
(10) Xu, M.; Zhang, T.; Gu, B.; Wu, J.; Chen, Q. *Macromolecules* **2006**, *39*, 354–355.
(11) Shanmugharaj, A. M.; Bae, J. H.; Nayak, R. R.; Ryu, S. H. *J. Polym. Sci., Part A* **2007**, *45*, 460–470.
(12) Gao, C.; Muthukrishnan, S.; Li, W.; Yuan, J.; Xu, Y.; Muller, H. E. *Macromolecules* **2007**, *40*, 1803–1815.
(13) Chen, J.; Hamon, M. A.; Hu, H.; Chen, Y.; Rao, A. M.; Eklund, P. C.; Haddon, R. C. *Science* **1998**, *282*, 95–98.
(14) Peng, H.; Alemany, L. B.; Margrave, J. L.; Khabashesku, V. N. *J. Am. Chem. Soc.* **2003**, *125*, 15174–15182.
(15) Williams, K. A.; Veenhuizen, T. M.; Torre, G.; Eritja, R.; Dekker, C. *Nature* **2002**, *420*, 761.
(16) Ogino, S.; Sato, Y.; Yamamoto, G.; Sasamori, K.; Kimura, H.; Hashida, T.; Motomiya, K.; Jeyadevan, B.; Tohji, K. *J. Phys. Chem. B* **2006**, *110*, 23159–23163.
(17) Matarredona, O.; Rhoads, H.; Li, Z.; Harwell, J. H.; Balzano, L.; Resasco, D. E. *J. Phys. Chem. B* **2003**, *107*, 13357–13367.
(18) Islam, M. F.; Rojas, E.; Bergey, D. M.; Johnson, A. T.; Yodh, A. G. *Nano Lett.* **2003**, *3*, 269–273.
(19) Vaisman, L.; Wagner, H. D.; Marom, G. *Adv. Colloid Interface Sci.* **2006**, *128*, 37–46.
(20) O'Connell, M. J.; Boul, P.; Ericson, L. M.; Huffman, C.; Wang, Y.; Haroz, E.; Kuper, C.; Tour, J.; Ausman, K.; Smalley, R. E. *Chem. Phys. Lett.* **2001**, *342*, 265–271.
(21) Sinani, V. A.; Gheith, M. K.; Yaroslavov, A. A.; Rakhnyanskaya, A. A.; Sun, K.; Mamedov, A. A.; Wicksted, J. P.; Kotov, N. A. *J. Am. Chem. Soc.* **2005**, *127*, 3463–3472.
(22) Li, C. Y.; Li, L.; Cai, W.; Kodjie, S. L.; Tenneti, K. K. *Adv. Mater.* **2005**, *17*, 1198–1202.
(23) Zheng, M.; Jagota, A.; Strano, M. S.; Santos, A. P.; Barone, P. S.; Chou, G.; Diner, B. A.; Dresselhaus, M. S.; Mclean, R. S.; Onoa, G. B.; Samsonidze, G. G.; Semke, E. D.; Usrey, M.; Walls, D. J. *Science* **2003**, *302*, 1545–1548.
(24) Dieckmann, G. R.; Dalton, A. B.; Johnson, P. A.; Razal, J.; Chen, J.; Giordano, G. M.; Muñoz, E.; Musselman, I. H.; Baughman, R. H.; Draper, R. K. *J. Am. Chem. Soc.* **2003**, *125*, 1770–1777.
(25) Nicolosi, V.; Cathcart, H.; Dalton, A. R.; Aherne, D.; Dieckmann, G. R.; Coleman, J. N. *Biomacromolecules* **2008**, *9*, 598–602.
(26) Fukushima, T.; Kosaka, A.; Ishimura, Y.; Yamamoto, T.; Takigawa, T.; Ishii, N.; Aida, T. *Science* **2003**, *300*, 2072–2074.
(27) Price, B. K.; Hudson, J. L.; Tour, J. M. *J. Am. Chem. Soc.* **2005**, *127*, 14867–14870.
(28) Pinnavaia, T. J. *Science* **1983**, *220*, 365–371.

(29) Lin, J. J.; Chen, Y. M. *Langumir* **2004**, *20*, 4261–4264.
(30) Rives, V.; Ulibarri, M. A. *Coord. Chem. Rev.* **1999**, *181*, 61−120.
(31) Rives, V. *Mater. Chem. Phys.* **2002**, *75*, 19–25.
(32) Chan, Y. N.; Juang, T. Y.; Liao, Y. L.; Dai, S. A.; Lin, J. J. *Polymer* **2008**, *49*, 4796–4801.
(33) Grossiord, N.; Regev, O.; Loos, J.; Meuldijk, J.; Koning, C. E. *Anal. Chem.* **2005**, *77*, 5135–5139.
(34) Yu, J.; Grossiord, N.; Koning, C. E.; Loos, J. *Carbon* **2007**, *45*, 618–623.
(35) Qin, Y.; Liu, L.; Shi, J.; Wu, W.; Zhang, J.; Guo, Z. X.; Li, Y.; Zhu, D. *Chem. Mater.* **2003**, *15*, 3256–3260.
(36) Baskaran, D.; Mays, J. W.; Bratcher, M. S. *Chem. Mater.* **2005**, *17*, 3389–3397.

JP9026805